Arab Journal of Physical Chemistry- http://aphyschem.org

Saudi Chemical Society

Article/ Maneechakr et al.

Biosorption of iodine and reactive dye using a new low cost *Ficus lyrata* seed powder adsorbent

Panya Maneechakr*, Jittima Samerjit, Siwarak Uppakarnrod, Surachai Karnjanakom**

Department of Chemistry, Faculty of Science, Rangsit University, Pathumthani 12000, Thailand

*Email: panya.m@rsu.ac.th and **email: surachaikarn@gmail.com

Received 03 March 2015,
Accepted 04 April 2015.

- **Novelty and Highlights:**

1 – *Ficus lyrata* seed powder was new low cost adsorbent, abundant and environmental friendly.

2 – *Ficus lyrata* seed powder was applied for removals of iodine and reactive dye from waste water model.

3 – Kinetic studies showed that the adsorption followed the pseudo-second order reaction.

- **Graphical Abstract:**

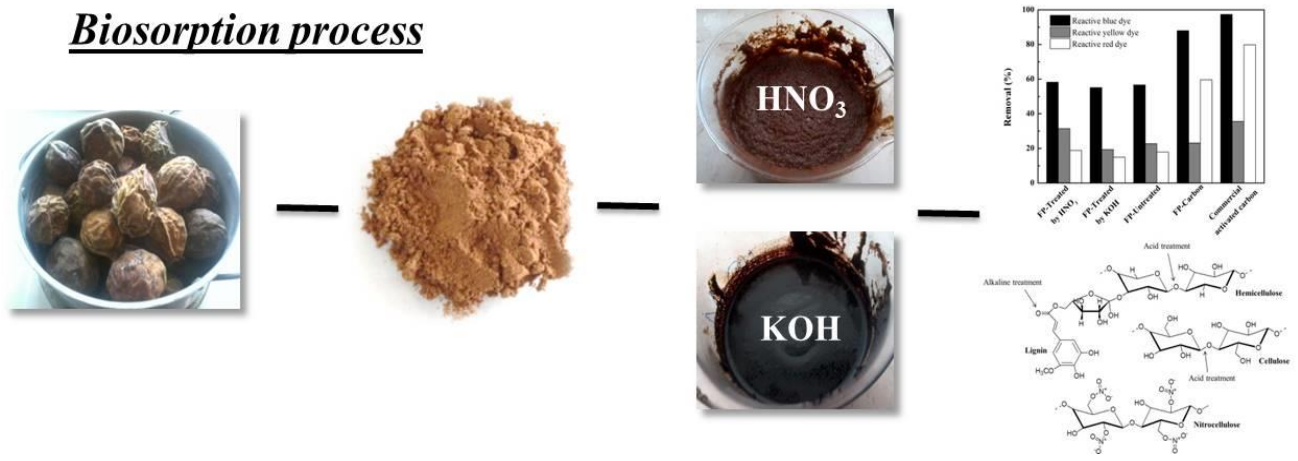

Arab Journal of Physical Chemistry- http://aphyschem.org

Saudi Chemical Society

Article/ Maneechakr et al.

Biosorption of iodine and reactive dye using a new low cost *Ficus lyrata* seed powder adsorbent

Panya Maneechakr*, Jittima Samerjit, Siwarak Uppakarnrod, Surachai Karnjanakom**

Department of Chemistry, Faculty of Science, Rangsit University, Pathumthani 12000, Thailand

*E-mail: panya.m@rsu.ac.th and **E-mail: surachaikarn@gmail.com

Abstract: A new adsorbent as a *Ficus lyrata* seed powder (FP) was applied for removal of iodine and reactive dyes in waste water model. FP was treated by chemicals with 10 %w/v HNO_3 (FP-Treated by HNO_3) and 10 %w/v KOH (FP-Treated by KOH). Specific surface area of adsorbent was quantified by adsorption of methylene blue together with using Langmuir isotherm. The result showed that specific surface area of FP-Treated by HNO_3, FP-Treated by KOH and FP-Untreated were 19.42, 18.47 and 18.71 m^2/g, respectively. The properties of adsorbent as adsorption capacities depended on the type of chemical agent and activated condition. Batch experiment of adsorption was carried out by different conditions as absorbent amount and dye concentration using iodine and reactive blue)RB(dye adsorbates. Adsorption data were modeled using the Langmuir and Freundlich isotherms by considering the correlation coefficient (R^2). Adsorption kinetic data were verified using pseudo-first order and pseudo-second order. Kinetic studies showed that the adsorption followed the pseudo-second order reaction.

Keywords: Biosorption, iodine, dye, Ficus lyrata seed.

Introduction

Nowadays, removal of dye from waste water is a major environment problem. Moreover, it is the first contamination to be recognized in nature of water. Some kind of dye also found to mutagenic for bacteria, yeast and mammalian somatic cells, toxic to female reproductive system, crosses the human placenta and excreted in human breast milk when applied to eyes as a topical opthalmic solution [1,2]. Dyes are complex aromatic molecular structure and present generally resistant to light, temperature and oxidizers. This characteristic feature makes the dye non-degradable and therefore causes bioaccumulation in living organisms, leading to severe diseases and disorders. In general, synthetic dyes and pigments are extensively used in many industries, i.e., printing, dyeing, textiles, paper, cosmetics, food, etc. to color their products, resulting in generation of waste water as high organic color content [3,4]. Molecule of iodine is found as one of major species that can be seen in food drink water and seawater sources. Moreover, iodine is also one part of fission products generated in a nuclear reactor, suggesting that it can enter into the reactor water [5].

The removal of dye and iodine toxics has been focused in present. Many methods for removal of these toxics have been identified, i.e., adsorption, coagulation, precipitation, photo-catalytic, ozonization, microbial decomposition, electrochemical, etc. [6]. Most promising method for removal of toxics is an adsorption method due to low cost, green process as well as eco-friendly. Activated carbon as an adsorbent is used extensively due to excellent toxic removal efficiency [7]. However, using of activated carbon is limited because its expensive. As well known that activated carbon was prepared via high temperature system in the presence of steam, air, nitrogen and CO_2 as well as using chemical activation, indicating that high cost for preparation required. Therefore, researchers look out for low cost adsorbent materials for as replaces to activated carbon. The probability of cheaper adsorbent materials, i.e., coconut husk, spent tea leaves, orange peel, wheat bran, etc. have investigated for removal of chemicals from wastewater [8-10]. Interestingly, activated carbon is a structure containing of linkage of carbon bond (C-C) which is non-polar molecule structure, while adsorbent biomass material without calcination mainly consists of cellulose, hemicellulose and lignin as well as many hydroxyl group (O-H) and carbonyl group (C=O) on surface structure which is polar molecule. This is likely to see the different

selectivity between type of adsorbent and type of adsorbate.

To date, no study has been reported on removal of wastewater using *Ficus lyrata* adsorbent. *Ficus lyrata* seed was produced from tree and not utilized which mostly go to waste. In this work, FP as a new low cost adsorbent material was used for removal of iodine and reactive dye from waste water model. FP was prepared by chemical treatments with HNO_3 and KOH solutions without carrying out at high temperature and pressure. A few works using at ambient temperatures and atmospheric pressure can be found, whereas it has various merits such as the possibility of simplification of equipment and avoiding unnecessary heating. Isotherm and kinetic adsorption were investigated to evaluate experimental data. The obtained results are expected to further apply in commercial industries.

Experimental

Preparation of Ficus lyrata seed powder *Ficus lyrata* seed was collected from Pathumthani, Thailand and used as an adsorbent. *Ficus lyrata* seed was crushed using a ball mill, sieved using a sieve 50 mesh and dried in oven at 105 °C. Proximate analysis was determined following on ASTM D2867-95 and D2866 -94. The result of proximate analysis is shown in **Table 1**. For treatment process, FP was treated by 10% HNO_3 (J.T. Baker, USA) and 10% KOH (J.T. Baker, USA) chemical solution. Initially, 20 g of FP was added in 50 mL of 10% chemical solution. Soaking for 24 h at ambient temperatures and atmospheric pressure was carried out. After the soaking, FP-treated was repeatedly washed using DI water until pH become neutral and dried at 105 °C.

Table 1 Proximate analysis of *Ficus lyrata* powder.

Adsorbent	Proximate analysis (wt.%)			
	Moisture	Volatile matter	Ash	Fixed carbon[a]
Ficus lyrata powder	22.59	65.96	0.93	10.52

[a] mass difference

Adsorption isotherm and kinetic studies of iodine The experiment was carried out by batch adsorption method. The adsorption isotherm was carried out with different amounts of adsorbent from 0.25 to 2 g by keeping 25 mL of 0.1N iodine (Univar, Analytical grade) and 150 rpm of agitation speed for 30 min of contact time constants. The adsorption kinetic was carried out by varying time from 0 to 30 min. The initial and residual concentrations of iodine were determined by titration method with 0.1N sodium thiosulfate titrant (Univar, Analytical grade).

Adsorption isotherm and kinetic studies of reactive blue dye The adsorption isotherm was done with 25 mL of initial concentration of reactive blue dye (Reactive blue 19, Mw = 502 g/mol) from 5 to 40 ppm by keeping 0.25 g of adsorbent and 150 rpm of agitation speed for 30 min of contact time constants. The adsorption kinetic was carried out by varying time from 0 to 30 min. The initial and residual concentrations of reactive blue dye were measured at 580 nm using spectrophotometer (GENESYS™ 20, USA). The chemical structure of reactive blue dye is shown in **Fig. 1**.

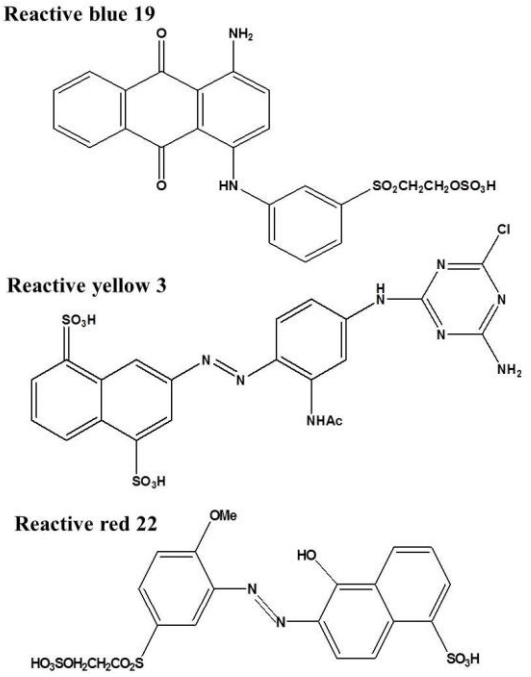

Fig. 1 Chemical structures of reactive dyes.

The equilibrium adsorption capacity and percentage removal of adsorbate were calculated by the following **Eqs. (1)** and **(2)**, respectively:

$$q_e = (C_i - C_e)\frac{V}{M} \quad (1)$$

$$\% \text{ Removal} = \frac{C_i - C_e}{C_i} \times 100 \quad (2)$$

where q_e is the equilibrium adsorption capacity (mg/g), C_i and C_e are the initial and equilibrium concentrations of adsorbate (mg/L), respectively, V is the volume of adsorbate solution (L) and M is the mass of adsorbent (g). The results of each

experiment were averaged from three time measurements.

Langmuir adsorption isotherm of methylene blue in this work, the surface area of adsorbent was determined from Langmuir isotherm model with based on maximum monolayer adsorption capacity. A schematic of interaction between methylene blue and FP is shown in **Fig. 2**.

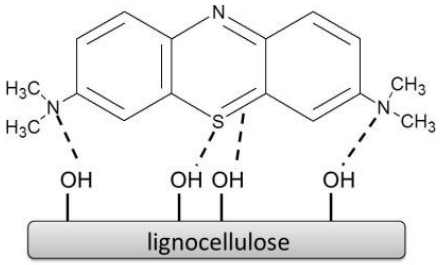

Fig. 2 Schematic model of adsorption interaction between methylene blue and *Ficus lyrata* seed powder.

The specific surface area can be calculated by following **Eq. (3)**:

$$S = \frac{Q_0 \times N \times a_{MB}}{n} \qquad (3)$$

where S is the specific surface area (m^2/g), Q_0 is the maximum monolayer adsorption capacity (mol/g), N is the Avogadro's number (6.02×10^{23} mol^{-1}), a_{MB} is the occupied surface area of one molecule of methylene blue (197.2 $Å^2$) and n is the amount of aggregation of methylene blue (n = 2.5).

Results and discussion,

Adsorption isotherms of iodine **Fig. 3** shows effect of amount of adsorbent on iodine removal efficiency. It can be seen that removal percentage of iodine increased as increasing amount of adsorbent, resulting from increase of adsorbent surface and availability of more adsorption sites [11]. However, it should be noted that excessive amount of adsorbent could lead to decrease of adsorption capacity due to aggregation of adsorption sites resulting in a decrease of surface area of adsorbent while diffusion path length increased. In expectation of this work, using chemical treatment, surface properties of adsorbent was changed, leading to increase adsorption efficiency.

As shown in **Fig. 4**, as well known that acid treatment is a process to break the rigid structure of lignocellulosic biomass in which hydronium ions breakdown and attack intermolecular bonds among cellulose, hemicellulose, and lignin in biomass hierarchy structure (It was related to the breakage of β-1,4 glycosidic bonds in cellulose.) [12].

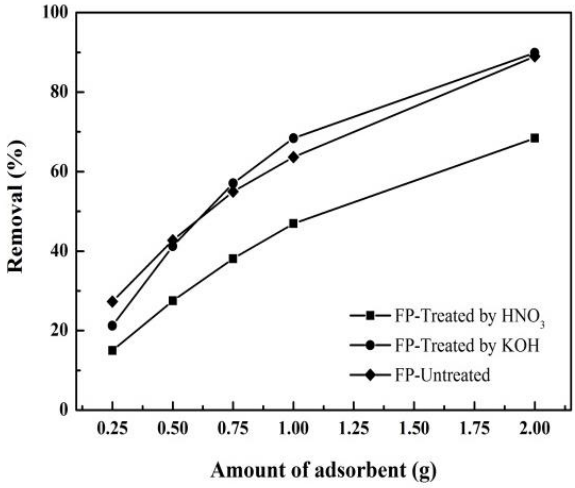

Fig. 3 Effect of amount of adsorbent on iodine removal efficiency using 25 mL of 0.1N iodine concentration, 30 min of contract time and 0.25 to 2 g of adsorbents.

For alkaline treatment, it is to disrupt the lignin structure in biomass. The mechanism involves saponification of intermolecular ester bond, which crosslinks xylan (hemicellulose) and lignin [13]. However, as shown in **Fig. 3**, FP-Untreated presents higher iodine removal efficiency than FP-Treated, especially in FP-Treated by HNO_3.

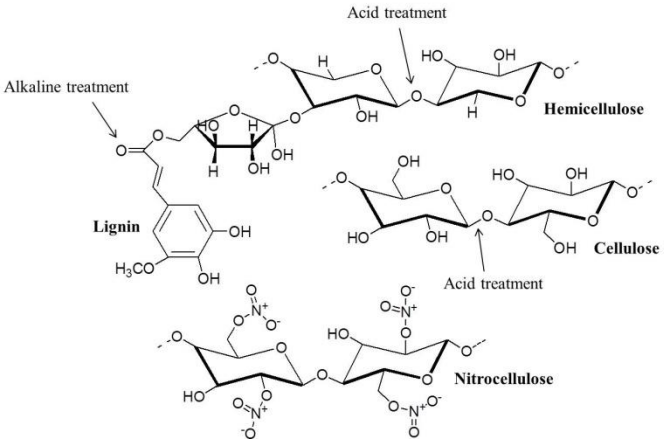

Fig. 4 Selectivity of chemical treatment for lignocellulosic biomass and formation of nitrate group on lignocellulosic biomass.

This was due to relationship between polarity and non-polarity. Iodine is non-polar molecule (C-C). In contrast, adsorbent in this work contains mostly of functional groups as hydroxyl and carbonyl. Moreover, during treatment by HNO_3, it is possible that esterification process could be occurred between nitrate

groups and hydroxyl groups to yield "nitrocellulose" which resulted in negatively charged surface of the cellulose crystallites (**Fig. 4**) [14]. Also, swelling of cellulose affected to increase of adsorption site.

The equilibrium relationships between adsorbent and adsorbate can be explained by the adsorption isotherms [15,16]. Based on ideal assumption of a monolayer adsorption, Langmuir isotherm model has been successfully applied to many true adsorption processes and is commonly expressed by following **Eq. (4)**:

$$q_e = Q_0 \frac{K_L C_e}{1 + K_L C_e} \qquad (4)$$

The linear transformation of Langmuir isotherm is expressed by following **Eq. (5)**:

$$\frac{C_e}{q_e} = \frac{1}{Q_0 K_L} + \frac{C_e}{Q_0} \qquad (5)$$

where C_e is the equilibrium concentrations of adsorbate (mg/L), qe is the equilibrium adsorption capacity (mg/g), Q_0 is the maximum monolayer adsorption capacity (mg/g) and K_L is the Langmuir constant related to affinity of the binding sites and energy of adsorption (L/mg). When C_e/q_e was plotted against C_e, a straight line with the slope of $1/Q_0$ and intercept of $1/ Q_0K_L$ were obtained (figure is not included).

Freundlich isotherm model was described to be multilayer adsorption. It is expressed by following **Eq. (6)**:

$$q_e = K_F C_e^{\frac{1}{n}} \qquad (6)$$

The linear logarithmic form of the Freundlich isotherm can be expressed by following **Eq. (7)**:

$$\log q_e = \log K_F + \frac{1}{n} \log C_e \qquad (7)$$

where K_F is the Freundlich constant related to the adsorption capacity [mg/g(L/mg)$^{1/n}$] and $1/n$ is the intensity of adsorption and constants incorporating the factors affecting the adsorption capacity. A plot of log q_e versus log C_e, where the values of K_F and $1/n$ were obtained from the intercept and slope of straight line (figure is not included).

The constant values of Q_0, K_L, K_F and $1/n$ for adsorption of iodine were calculated and presented in **Table 2**. The obtained highest constant values of Q_0 and K_F were 370 mg/g and 8.0872 mg/g(L/mg)$^{1/n}$, respectively using FP-Untreated adsorbent, indicating that FP-Untreated adsorbent exhibits iodine adsorption capacity better than FP-treated. The R_L value was calculated from C_0 and K_L and found in range of favorable ($0 < R_L < 1$) uptake process of iodine adsorption.

Table 2 Fitted parameters of Langmuir and Freundlich isotherms on iodine adsorption.

Adsorbent	Langmuir isotherm model			Freundich isotherm model		
	Q_0 (mg/g)	K_L (L/mg)	R^2	K_F	$1/n$	R^2
FP-HNO_3	124.55	0.00033	0.9974	0.7173	0.5558	0.9928
FP-KOH	119.05	0.00162	0.9988	7.4611	0.3234	0.9803
FP	370.37	0.00040	0.8938	8.0872	0.3913	0.9576

The values of $1/n < 1$ (a normal Freundlich isotherm) indicate slowly increase of qe when C_e was increased, suggesting that the magnitude of the term $(1/n)$ gives an indication of the favorability of the adsorbent/adsorbate systems while $1/n > 1$ is indicative of cooperative adsorption [17]. As shown in **Table 2**, FP-Treated by HNO_3 and KOH were fitted with Langmuir isotherm model which contrast with FP-Untreated. This indicates that FP-Treated by HNO_3 and KOH could adsorb iodine in style of monolayer as well as chemisorption.

Adsorption kinetics of iodine the adsorption kinetics of iodine is required for operating conditions for the full-scale batch. It was used for prediction of adsorption rate, giving important information for modeling the adsorption processes [18]. In order to investigate the mechanism of adsorption, Lagergren pseudo-first-order, Ho and Mckay pseudo-second-order kinetic models have been used for all experimental data. The pseudo-first-order linear model and pseudo-second-order linear model are given according to Eqs. (8) and (9), respectively:

$$\log (q_e - q_t) = \log q_e - \frac{k_1}{2.303} t \qquad (8)$$

$$\frac{t}{q_t} = \frac{1}{k_2 q_e^2} + \frac{t}{q_e} \qquad (9)$$

where q_t and q_e are the adsorption capacity at time t and equilibrium adsorption capacity (mg/g), respectively, k_1 and k_2 are the rate constant of adsorption of pseudo-first-order and pseudo-first-order (min^{-1}), respectively, t is the adsorption time (min).

The plots of t/q_t versus t are shown in **Fig. 5**. Kinetic constants were determined from slope and intercept for both the models and listed in **Table 3**.

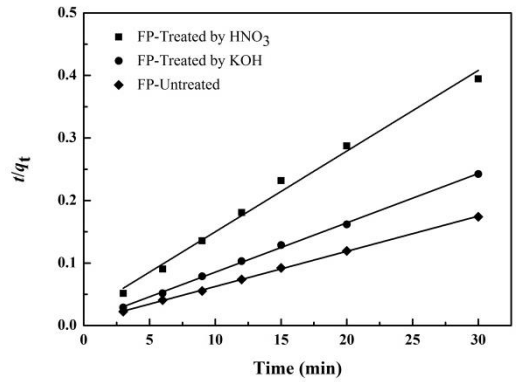

Fig. 5 Pseudo-second-order kinetic model on iodine removal efficiency with different adsorbents.

It should be noted that the validity of model was checked by fitness of the straight line (R^2) and comparing between the experimental and calculated values of q_e. From the result, it was clearly found that R^2 of pseudo-second-order model is significant, indicating that this model was fitted. Also, the calculated q_e values were closed with the experimental data very well. R^2 of pseudo-first-order model is not significant and that is why the figure of this is not shown.

Table 3 Pseudo-first-order and pseudo-second-order kinetic model parameters on iodine adsorption.

Adsorbent	$q_{e,exp}$ (mg/g)	Pseudo-first-order			Pseudo-second-order		
		$q_{e,calc}$	k_1 (min^{-1})	R^2	$q_{e,calc}$	k_2 (min^{-1})	R^2
$FP-HNO_3$	77.66	26.07	0.0784	0.8095	77.52	0.0080	0.9916
FP-KOH	131.06	24.66	0.0454	0.8040	126.58	0.0090	0.9989
FP	182.02	43.19	0.1237	0.8678	178.57	0.0051	0.9996

The highest rate constant value of pseudo-second-order model was 0.009 min^{-1} which obtained from FP-Treated by KOH, suggesting that initial rate adsorption of FP-Treated KOH is faster when compared with FP-Treated by HNO_3 and FP-Untreated.

Adsorption isotherms of reactive blue dye Fig. 6 shows the effect of dye concentration on reactive blue dye removal efficiency. A dramatic decrease in the removal efficiency of reactive blue dye as initial dye concentration increased from 5 to 40 ppm obtained. This trend was due to the fact that for a fixed adsorbent amount, the total available adsorption sites were limited, which become saturated with using a higher adsorbate concentration [19].

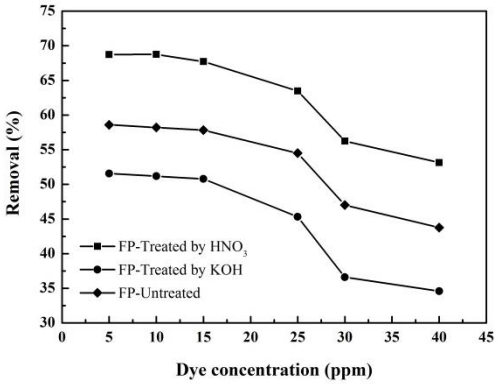

Fig. 6 Effect of dye concentration on reactive blue dye removal efficiency using 0.25 g of adsorbent, 30 min of contract time and 25 mL of reactive blue dye with different concentration of 5 to 40 ppm.

Interestingly, as shown in **Fig. 6**, FP-Treated by HNO_3 gives highest reactive blue dye removal efficiency, suggesting that FP-Treated by HNO_3 was successfully prepared due to the enhancement of interaction between the adsorbent and reactive dye. Moreover, it can be explained to charge increasing on adsorbent surface after treatment by HNO_3, which this increased charge could enhances interaction efficiency of reactive dye involving based on theoretical electric charge and polarity adsorption mechanism. The lowest reactive blue dye removal percentage was obtained using FP-Treated by KOH. It is possible that the FP structure was destroyed as KOH utilized. Moreover, cellulose can also be converted to salt as following:

$$C_6H_{10}O_5 + 12KOH + H_2O \rightarrow 6K_2CO_3 + 12H_2 \quad (10)$$

The parameters of adsorption isotherm for reactive blue dye are summarized in **Table 4**. It was found that the Freundlich isotherm model was obviously the most appropriate for FP-Treated by HNO_3 and KOH due to its high R^2 relative, which described the reactive blue dye adsorption process as the multilayer style. FP-Untreated was found to be closed Langmuir isotherm model. The constant values of isotherms exhibited to relate corresponding with adsorption capacity.

Adsorption kinetics of reactive blue dye **Fig. 7** shows the plots of t/q_t versus t for pseudo-second-order. The adsorption rate constant of reactive blue dye for both kinetic models are summarized in **Table 5**.

Table 4 Fitted parameters of Langmuir and Freundlich isotherms on reactive blue dye adsorption.

Adsorbent	Langmuir isotherm model			Freundich isotherm model		
	Q_0 (mg/g)	K_L (L/mg)	R^2	K_F	1/n	R^2
FP-HNO_3	3.596	0.0715	0.9609	0.2796	0.7176	0.9663
FP-KOH	2.078	0.0671	0.9639	0.1774	0.6455	0.9674
FP	3.2446	0.0529	0.9848	0.2015	0.7255	0.9831

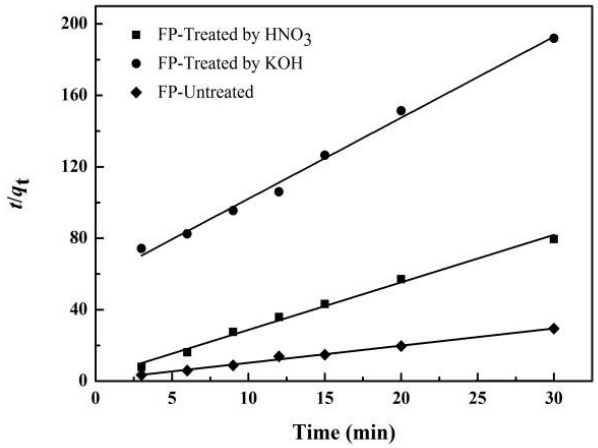

Fig. 7 Pseudo-second-order kinetic model on reactive blue dye removal efficiency with different adsorbents.

The results show that pseudo-second-order model could descried the kinetics of reactive blue dye adsorption due to high R^2 closer to 1, as well as calculated q_e values agreed with the experimental data very well for almost all the cases. This indicates that the adsorption of reactive blue dyes onto these adsorbents followed the pseudo second-order model.

Table 5 Pseudo-first-order and pseudo-second-order kinetic model parameters on reactive blue dye adsorption.

Adsorbent	$q_{e,exp}$ (mg/g)	Pseudo-first-order			Pseudo-second-order		
		$q_{e,calc}$	k_1 (min^{-1})	R^2	$q_{e,calc}$	k_2 (min^{-1})	R^2
FP-HNO_3	0.38	0.02	0.0293	0.0525	0.38	3.3842	0.9933
FP-KOH	0.16	0.17	0.0962	0.9757	0.22	0.3636	0.9935
FP	1.02	0.04	0.0930	0.1977	1.04	1.4668	0.9925

Adsorption of synthetic wastewater

To understand more adsorption mechanism process, synthetic wastewater model was tested. Synthetic wastewater was prepared by mixing of reactive blue 19 (Mw = 502 g/mol and λ_{max} = 580 nm), reactive yellow 3 (Mw = 608.5 g/mol and λ_{max} = 422.5 nm) and reactive red 22 (Mw = 514 g/mol and λ_{max} = 490.5 nm) dyes together at each 5 ppm of concentration. The initial and residual concentrations of synthetic wastewater were measured at 580, 422.5 and 490.5 nm, and calculated by matrix method with Cramer's rule. To compare, the chemical structures of three reactive dyes are shown in **Fig. 1**. The adsorption was carried out using 25 mL of 5 ppm synthetic waste water concentration 0.5 g of adsorbent and 150 rpm of agitation speed for 30 min of contact time. FP-Untreated and FP-Treated by HNO_3 and KOH were used to test for the adsorption of synthetic wastewater. Moreover, carbon preparing from FP was also tested. The condition for carbon preparation was carried out at 400 °C for 3 h for calcination. The surface areas of these adsorbents are given in **Table 6**.

Table 6 The specific surface areas of adsorbents determining from methylene blue adsorption.

Adsorbent	Q_0 (mol/g)	R^2	Surface area (m^2/g)
FP-HNO_3	4.09×10^{-5}	0.9869	19.42
FP-KOH	3.89×10^{-5}	0.9825	18.47
FP	3.94×10^{-5}	0.9847	18.71
FP-Carbon	4.53×10^{-5}	0.9850	21.51
Commercial carbon	1.81×10^{-3}	0.9980	524.33

As shown in **Fig. 9**, the commercial carbon (Fluka, Analytical grade) shows highest removal percentage of three types of reactive dyes. The removal percentages of reactive blue, reactive yellow and reactive red dyes using commercial carbon adsorbent were 97.35, 35.59 and 79.83%, respectively. The reactive blue dye was easier adsorbed than other reactive dyes because of the chemical structure of reactive blue dye has smaller size than other reactive dyes. In general, adsorption by mass force between carbon and dye was occurred. So, structure size of dye has influence to adsorption.

In case of FP-Treated by HNO_3, removal percentages of reactive blue, reactive yellow and reactive red dyes were 58.25, 31.47 and 18.91%, respectively and were higher than when compared with FP-Treated by KOH and FP-Untreated. One can see that using FP adsorbents, reactive yellow dye adsorbed better than reactive red dye although structure size of reactive red dye was smaller. It should be noted that they related between mass force and charge force as well as polarity with surface area on theoretical adsorption [20]

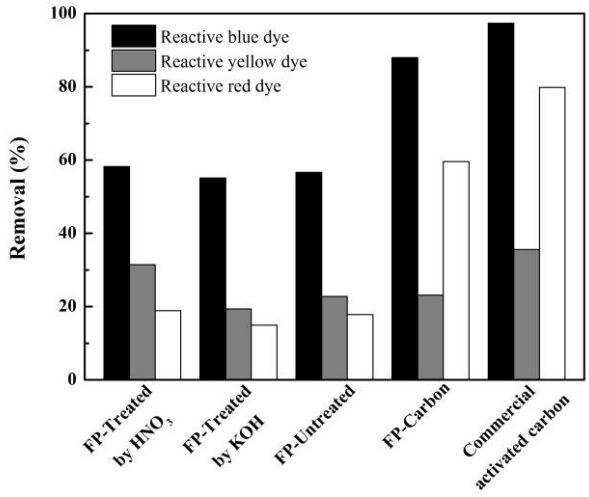

Fig. 9 Removal of synthetic waste water by different adsorbents using 25 mL of 5 ppm synthetic waste water concentration, 30 min of contract time and 0.5 g of adsorbent.

Conclusions

FP was successfully applied as a low cost alternative adsorbent for the removal of iodine and reactive dye. FP-Treated by HNO_3 was found to suitable with adsorption of reactive dye while FP-Untreated provided a good result with adsorption of iodine. The Adsorption equilibrium data were well-fitted to isotherm models. Adsorption of iodine and reactive blue dye on all studied adsorbents followed the pseudo second-order model. Finally, it can therefore be concluded that novel FP offers promise as an economically viable alternative. However, high mount of FP was required when compared with commercial carbon.

Acknowledgements

The authors wish to acknowledge the Department of Chemistry, Faculty of Science, Rangsit University for supporting all instruments and chemicals. J. Samerjit, S. Uppakarnrod and S. Karnjanakom are grateful to Assistant Professor P. Maneechakr for his valuable suggestions.

Notes and references

1. D.B. Jirekar and M. Farooqui, *Arab J. Phys. Chem.*, 2015, **1**, 1.
2. M. Ghaedi, A.M. Ghaedi, M. Hossainpour, A. Ansari, M.H. Habibi and A.R. Asghari, *J. Ind. Eng. Chem.*, 2014, **20**, 1641.
3. J. Galán, A. Rodríguez, J.M. Gómez, S.J. Allen and G.M. Walker, *Chem. Eng. J.*, 2013, **219**, 62.
4. G. Annadurai, L.Y. Ling and J.F. Lee, *J. Hazard. Mater.*, 2008, **152**, 337.
5. J. Zhou, S. Hao, L. Gao and Y. Zhang, Ann. Nucl. Energy, 2014, **72**, 237.
6. K.G. Akpomie and F.A. Dawodu, *J. Taibah. Univ. Sci.*, 2014, **8**, 343.
7. M.M. Lakdawala and Y.S. Patel, *Arab J. Phys. Chem.*, 2014, **1**, 8.
8. M. Arami, N.Y. Limaee, N.M. Mahmoodi and N.S. Tabrizi, *J. Colloid Interface Sci.*, 2005, **288**, 371.
9. M.T. Sulak, E. Demirbas and M. Kobya, *Bioresour. Technol.*, 2007, **98**, 2590.
10. N. Nasuha, B.H. Hameed and A.T.M. Din, *J. Hazard. Mater.*, 2010, **175**, 126.
11. G.M. Nabil, N.M. El-Mallah and M.E. Mahmoud, *J. Ind. Eng. Chem.*, 2014, **20**, 994.
12. P. Gao, G. Li, F. Yang, X.N. Lv, H. Fan, L. Meng and X.Q. Yu, *Ind. Crops Prod.*, 2013, **48**, 61.
13. R. Zuluaga, J.L. Putaux, J. Cruz, J. Vélez, I. Mondragon and P. Gañán, *Carbohydr. Polym.*, 2009, **79**, 51.
14. M. Moniruzzaman, J.M. Bellerby and M.A. Bohn, *Polym. Degrad. Stab.*, 2014, **102**, 49.
15. M.E.K. Saad, R. Khiari, E. Elaloui and Y. Moussaoui, *Arabian J. Chem.*, 2014, **7**, 109.
16. M.D. Meitei and M.N.V. Prasad, *Ecol. Eng.*, 2014, **71**, 308.
17. N.K. Amin, *Desalination*, 2008, **223**, 152.
18. D. Pathania, S. Sharma and P. Singh, *Arabian J. Chem.*, 2013, http://dx.doi.org/10.1016/j.arabjc.2013.04.021.
19. A.K. Yadav, R. Abbassi, A. Gupta and M. Dadashzadeh, *Ecol. Eng.*, 2013, **52**, 211.
20. M. Ghaedi, and N. Mosallanejad, *J. Ind. Eng. Chem.*, 2014, **20**, 1085.